# magnetic Resonance in Solids

## Electronic Journal
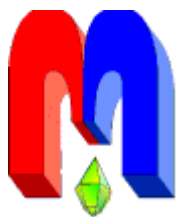
# Investigation of molecular mobility and exchange of n-hexane and water in silicalite-1 by 2D $^1$H NMR relaxometry

B.I. Gizatullin[1,2], A.V. Savinkov [1,*], T.V. Shipunov [1], D.L. Melnikova [1],
M.M. Doroginitzky [1], V.D. Skirda [1]

[1] Kazan Federal University, Kremlevskaya 18, Kazan 420008, Russia

[2] Ilmenau Technical University, Unterpoerlitzer 38, Ilmenau 98693, Germany

*\*E-mail: andrey.savinkov@gmail.com*

Molecular mobility and exchange of adsorbed fluid in porous media of silicalite-1 were studied by two-dimensional nuclear magnetic resonance (NMR) techniques in fully and partly saturated samples. Three porous volumes were determined in silicalite-1 where n-hexane and water molecules are adsorbed: intracrystallite channels, mesopores and intercrystallite space. The molecular exchange between all porous volumes was observed and typical exchange times were estimated for n-hexane and water. Using the exchange times the self-diffusion coefficients were estimated as $D \sim 1.11 \times 10^{-10}$ for n-hexane and $D \sim 6.67 \times 10^{-11}$ m$^2$/s for water in fully saturated silicalite-1 and found in a good agreement with literature data.

## 1. Introduction

The zeolites of the mordenite framework inverted (MFI) topology due to their unique properties have found wide application in the chemical industry in selective catalysis, adsorption and separation. Detailed study of the behavior of adsorbed fluids in zeolite pores is a subject of particular interest, since the dynamics and state of adsorbed molecules can have a close relation to the selective shape behavior exhibited by the zeolites [1-4].

The porous medium of MFI zeolites is rather complex and includes pores of different type and dimension (micropores, mesopores and macropores) that may give rise to rather different dynamics and behavior of adsorbed molecules in pores of different types. Moreover, due to high connectivity of the porous medium in zeolites the molecular transport occurs between different pores. Many experimental and theoretical works have been done to clarify the molecular mobility and state of adsorbed fluids in the porous medium of the MFI-type zeolites including synthetic high-silica zeolite ZSM-5 and silicalite-1 [5-10]. However, reported diffusion coefficients in MFI zeolites and properties of adsorbed molecules are often inconsistent. Usually, a simple two-phase model is used [11] to describe the diffusion coefficients, but MFI zeolites have a well-connected pore system of different pore types. Therefore it is natural to expect more complex diffusion, described by more advance models.

The MFI-type zeolites including aluminum free zeolites known as silicalite-1 have a three-dimensional system of intracrystallite pores, which are intersecting straight and zigzag channels. The straight channels aligning along *b*-axis of the crystallographic unit cell have a diameter of 5.4 Å by 5.6 Å, while the channels of second type follow a zig-zag path in the crystallographic ac-plane and have diameters of 5.1 Å by 5.4 Å [12]. The aluminum content determines the hydrophobicity of the MFI-zeolites [13], and has a significant effect on adsorption of polar molecules into intracrystallite pores. Studies of diffusion of methane in silicalite-1 [7, 9] and n-butane in ZSM-5 zeolites [7] revealed existence of intracrystallite transport barriers in MFI-type crystals. Authors of Ref. [7] suggested the intersections between different intergrowth components of MFI crystals and/or between the building blocks of the crystals as the diffusion barriers for guest molecules.

The MFI zeolites may also contain mesopores which include any intracrystallite pores with a typical size of 2 to 50 nm. Diffusivity through mesopores is much higher compared to the diffusivity in zeolite

intracrystallite channels [14, 15], hence the mesoporous zeolites have higher permeability and lower selectivity for guest molecules. Pore size, pore volume and connectivity of mesopores strongly depend on synthesis procedure and postsynthesis treatment (see review of the mesopore introduction methods in Ref. [16]). Zeolite samples also include macropores which are mainly the inter-crystallite pores with wide distributed size typically of 1-100 μm.

High hydrophobicity of the silicalite-1 intracrystallite channels leads to different adsorption capacity for various adsorbates. On one hand, organic fluids can penetrate into nano-sized intracrystallite channels (channels), but this is not the case for water molecules. Fluid molecules in channels under conditions of the highly restricted translation mobility are characterized by very fast transverse nuclear relaxation, so that $T_2$ values of $^1$H are less than tens of microseconds. Thus straight observation of nuclear magnetic resonance (NMR) signal corresponded to adsorbate molecules in channels is not possible in standard Pulsed Field Gradient (PFG) NMR experiments. On the other hand, water molecules as well as molecules of organic fluids located in big pores (mesopores, defects in crystallites, macropores) are characterized by transverse relaxation with low values of $T_2$ time.

Two-dimensional nuclear magnetic resonance relaxometry (2D NMR relaxometry) is one of the powerful methods to study the dynamic and exchange processes in porous media, such as mass transfer through space or magnetization transfer due to cross-relaxation and spin-diffusion. In this paper we present results of a detailed study of dynamical NMR-characteristics, molecular mobility and exchange of n-hexane and water adsorbed in silicalite-1 porous media by 2D $^1$H NMR relaxometry.
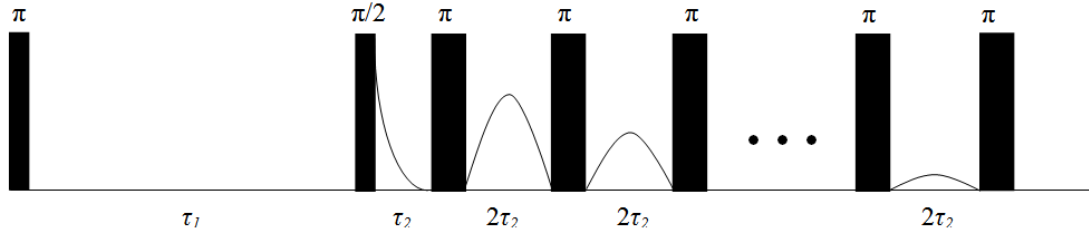
## 2. Experimental

Powder of Silicalite-1 was obtained from Lulea University of Technology (Sweden). The main preparation procedure of the silcalite-1 powder described in [10] includes a few stages. In the first stage, silicalite-1 crystals were prepared in fluoride media in the absence of hydroxyl ions to minimize the concentration of structural defects and silanol groups in the zeolite according to the procedure reported by Mostowicz et al. [17]. In fact, the synthesis was carried out in a Teflon-lined steel autoclave at 170°C for 18 hours using a synthesis mixture with a molar composition of: 10 NaF : 1.25 TPABr : 10 SiO$_2$ : 330 H$_2$O.

After synthesis, the zeolite crystals were collected and purified by repeated (four times) centrifugation and redispersion in distilled water. The crystals were subsequently dried at 60°C and then calcined at 550°C in air to remove the template molecules.

The silicalite-1 powder was placed in desiccator with n-hexane or water vapors for obtaining partially saturated samples. The desiccator with samples was vacuumed after the placing of the silicalite-1 powder. Amount of adsorbed liquid was controlled by weighting on the standard balance. The maximum of concentration of n-hexane and water adsorbed in silicalite-1 from a vapor at 298 K was 150 mg/g and 21 mg/g reached after 3 and 22.5 hours, correspondingly. Then obtained samples partially saturated by n-hexane and water were placed in 7.5 mm tube and sealed. Also, the mixing with bulk water or n-hexane with subsequent vacuuming were used for preparation of full liquid saturated samples. The concentrations of adsorbed n-hexane and water at full saturation were 680 and 795 mg/g, correspondingly. Thus we prepared four samples of silicalite-1, partially and fully saturated by n-hexane and water.

Pulsed NMR spectrometer Proton 20M (Chromatec ©) was used to measure the $^1$H magnetic relaxation. Main characteristics of the spectrometer are as following: radio-frequency is 20 MHz for $^1$H, duration of π/2 rf-pulse is 2.5 μs, dead time of receiver tract $\tau_p$ = 13 μs, inhomogeneity of the static magnetic field is not more than 0.01 gauss/cm. Measurements of relaxation times were performed at 298 K. The accuracy of measurements and stabilization of temperature was ±0.1 K.

The 2D NMR relaxation measurements provide a correlation between the initial (encoding) and final (decoding) parts of the NMR experiment. The encoding sequence may involve longitudinal $T_1$ recovery or transverse $T_2$ decay whereas decoding period involves the transverse $T_2$ decay providing the $T_1$-$T_2$ [18] or $T_2$-$T_2$ correlations in the sample. A specific approach to measure $T_1$-$T_2$ correlation maps as well as $T_2$-$T_2$ exchange maps includes a combined sequence for measuring FID and CPMG simultaneously

**Figure 1**. The pulse sequence used for the $T_1$-$T_2$ correlation experiments. Echo signals were detected after π-pulses. The phases used were, for the first π-pulse: 0°, for the π/2-pulse: 0°; and for the π-pulses in the CPMG train: 90°.
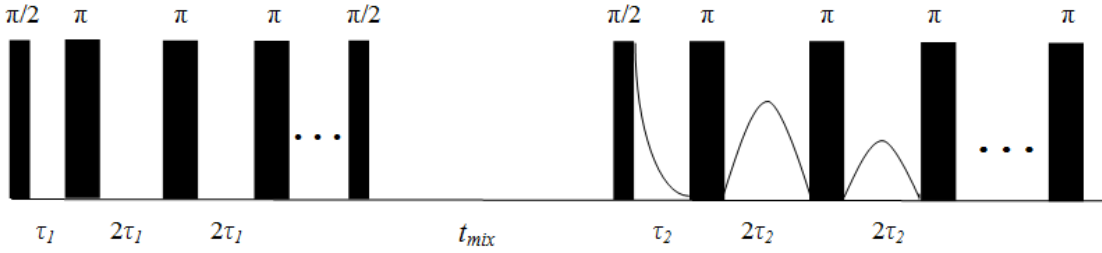


**Figure 2.** The pulse sequence used for the $T_2$-$T_2$ correlation experiments. Echo signals were detected in the decoding period after π-pulses divided by time interval of $2\tau_2$. In the encoding period the phases used were, for the first π/2-pulse: 0°, for π-pulses in the CPMG train: 90°, for the last π/2-pulse: 180°; in the decoding period for the π/2-pulse: 0°; and for the π-pulses in the CPMG train: 90°.

[19] (see Figures 1 and 2) that allows including in analysis the components of transverse relaxation with $T_2$ value less than 100 μs. The recovery time $\tau_1$ in the $T_1$-$T_2$ correlation sequence, and the echo time $\tau_2$, are two independent variables and the acquired data can be written as a two-dimensional array $A(\tau_1, \tau_2)$. Over the time period $\tau_1$, the spin magnetization recovers along the $z$-axis following a $T_1$ process. However, during $\tau_2$, the transverse spin magnetization decays due to a spin-spin relaxation process. This signal $A(\tau_1, \tau_2)$ is related to the $T_1$-$T_2$ joint distribution $P(T_1, T_2)$ through the 2D Fredholm integral of the first kind that describes the expected form of measured NMR data:

$$A(\tau_1,\tau_2) = \int_{T_{1,\min}}^{T_{1,\max}} \int_{T_{2,\min}}^{T_{2,\max}} dT_1 \, dT_2 \, K(\tau_1,\tau_2,T_1,T_2) P(T_1,T_2) + E(\tau_1,\tau_2). \tag{1}$$

Here $K(\tau_1, \tau_2, T_1, T_2)$ is the kernel function that describes the expected form of the NMR data, and $E(\tau_1, \tau_2)$ is experimental noise. Thus for the $T_1$-$T_2$ 2D NMR experiment the kernel function is given by:

$$K(\tau_1,\tau_2,T_1,T_2) = \left(1-2e^{-\tau_1/T_1}\right) \begin{Bmatrix} e^{-\left(\frac{\tau_2}{T_2}\right)^2} , & T_2 \leq T_{2\text{cutoff}} \\ e^{-\frac{\tau_2}{T_2}} , & T_2 > T_{2\text{cutoff}} \end{Bmatrix}. \tag{2}$$

The reference time $T_{2\text{cutoff}}$ is related to transition from "solid state" behavior of NMR signal with square exponential dependence to "liquid state" behavior characterized pure exponential decay [19]. The value of $T_{2\text{cutoff}} = 50$ μs was used in this study.

The pulse sequence for the two-dimensional $T_2$-$T_2$ correlation experiment based on the standard sequence including FID and CPMG as acquisition parts [19, 20] is presented in Figure 2. The $T_2$-encoding period consists of the CPMG pulse sequence where π-pulses are separated by $2\tau_1$ time intervals and single π/2-pulse (a phase is 180°) that keeps a nuclear magnetization along the $z$-axis, i.e. this π/2-pulse "cancels" the relaxation processes in the spin system. Then the exchange processes can occur during the variable mixing time $t_{\text{mix}}$ period. In the final decoding period the CPMG pulse sequence is used to detect the magnetization decay. The initial part of FID is also measured for detecting

components with $T_2$ times less than 100 μs. The detected NMR signal $A(\tau_1, \tau_2)$ related to the $T_2$-$T_2$ correlation function $P(T_2', T_2'')$ can be described through the 2D Fredholm integral:

$$A(\tau_1, \tau_2) = \int_{T_{2,\min}'}^{T_{2,\max}'} \int_{T_{2,\min}''}^{T_{2,\max}''} dT_2' \, dT_2'' \, K(\tau_1, \tau_2, T_2', T_2'') P(T_2', T_2'') + E(\tau_1, \tau_2). \tag{3}$$

The kernel function for the 2D $T_2$-$T_2$ correlation experiment is:

$$K(\tau_1, \tau_2, T_2', T_2'') = \left\{ \begin{array}{ll} e^{-\left(\frac{\tau_2}{T_2'}\right)^2}, & T_2' \le T_{2\text{cutoff}} \\ e^{-\frac{\tau_2}{T_2'}}, & T_2' > T_{2\text{cutoff}} \end{array} \right\} \cdot \left\{ \begin{array}{ll} e^{-\left(\frac{\tau_2}{T_2''}\right)^2}, & T_2'' \le T_{2\text{cutoff}} \\ e^{-\frac{\tau_2}{T_2''}}, & T_2'' > T_{2\text{cutoff}} \end{array} \right\}. \tag{4}$$

The equations (1) and (3) are solved numerically for the joint distribution $P(T_1, T_2)$ and correlation function $P(T_2', T_2'')$ using Tikhonov regularization [21, 22]. In the presence of noise a stable solutions are obtained applying restrictions of non-negative $T_1$ and $T_2$ times, finite values of the relaxation times (see integration bounds in eq. (1) and (3)) and applying that $T_1$ time is always exceeds $T_2$ (for the eq. (1)). Finally the relaxation $T_1$-$T_2$ correlation maps and $T_2$-$T_2$ exchange maps are obtained.

## 3. Results and discussion

### *Longitudinal and transverse relaxation of adsorbate in silicalite-1*

It was mentioned above that the porous structure of silicalite-1 [23] includes several types of pores. As a result, the $T_1$-$T_2$ correlation maps measured in the silicalite-1 samples (see Figure 3) show complicated patterns.

There are several well-resolved peaks on $T_1$-$T_2$ correlation maps measured in the silicalite-1 samples fully saturated by n-hexane (Figure 3a) and water (Figure 3c). Both saturated samples show three peaks (peaks "A", "B" and "C") characterized by a single spin-lattice relaxation time, but three different times of spin-spin relaxation. In the n-hexane saturated sample $T_1$ time is $1150 \pm 80$ ms; in the water-saturated sample $T_1$ is $680 \pm 30$ ms; $T_2$ times are in the wide range for both samples: about 0.08-40 ms and 0.03-200 ms in the samples, correspondingly. A low intensive peak "D" is observed in the $T_1$-$T_2$ map of n-hexane at full saturation with $T_1 \approx 85$ ms and $T_2 \approx 0.9$ ms. This value is close to $T_2$ value of other low intensive component marked as "B" peak in Figure 3a. In the water saturated sample the low intensive peak labeled as "B" corresponds to NMR signal with $T_1 \approx 650$ ms and $T_2 \approx 1$ ms (Figure 3c). The presence of several components on the $T_1$-$T_2$ maps may imply different restrictions on the mobility of adsorbed molecules in the silicalite-1 porous media. In both fully saturated samples the most intensive peak "C" (~80% of relative integral intensity on the $T_1$-$T_2$ maps) corresponds to n-hexane and water in intercrystallite porous space (intercrystallite porous volume) of silicalite-1 powder. Molecules of the fluids in the intercrystallite pores have the highest mobility.

A component "A" with the lowest value of $T_2 \approx 80$ μs for n-hexane and $T_2 \approx 30$ μs for water is attributed to the molecules in channels of silicalite-1 crystal [10, 24]. Strong restrictions of molecular mobility in the channels with diameter close to the critical diameter of the adsorbed molecules lead to dramatically decreasing of $T_2$ relaxation time. Furthermore, the relative parts of different porous volumes of silicalite-1 obtained by BET-analysis [10] are in good agreement with obtained relative intensities of the peaks on $T_1$-$T_2$ maps. However, according to Ref. [10] there should be an another porous volume in silicalite-1 attributed to mesopores with typical size of about 2-50 nm and relative total volume of ~0.5%. It is natural to suggest that the peaks "B" and "D" in the n-hexane sample and the "B" peak in the water-saturated sample with $T_2 \approx 0.9$ ms and relative intensity of about 0.5% is attributed to the fluid molecules adsorbed in mesopores. It is known that diagonal peaks or peaks parallel to the diagonal on $T_1$-$T_2$ maps (see peaks "C" and "D" in Figure 3a) form an additional cross-peak (presumably the peak "B") if an exchange of magnetization appears between porous volumes associated with diagonal peaks. Thus, we suggest that the "B" peak is caused by the molecular exchange between porous volumes corresponded to the mesopores and intercrystallite volume (see "C" and "D" peaks in Figure 3a).
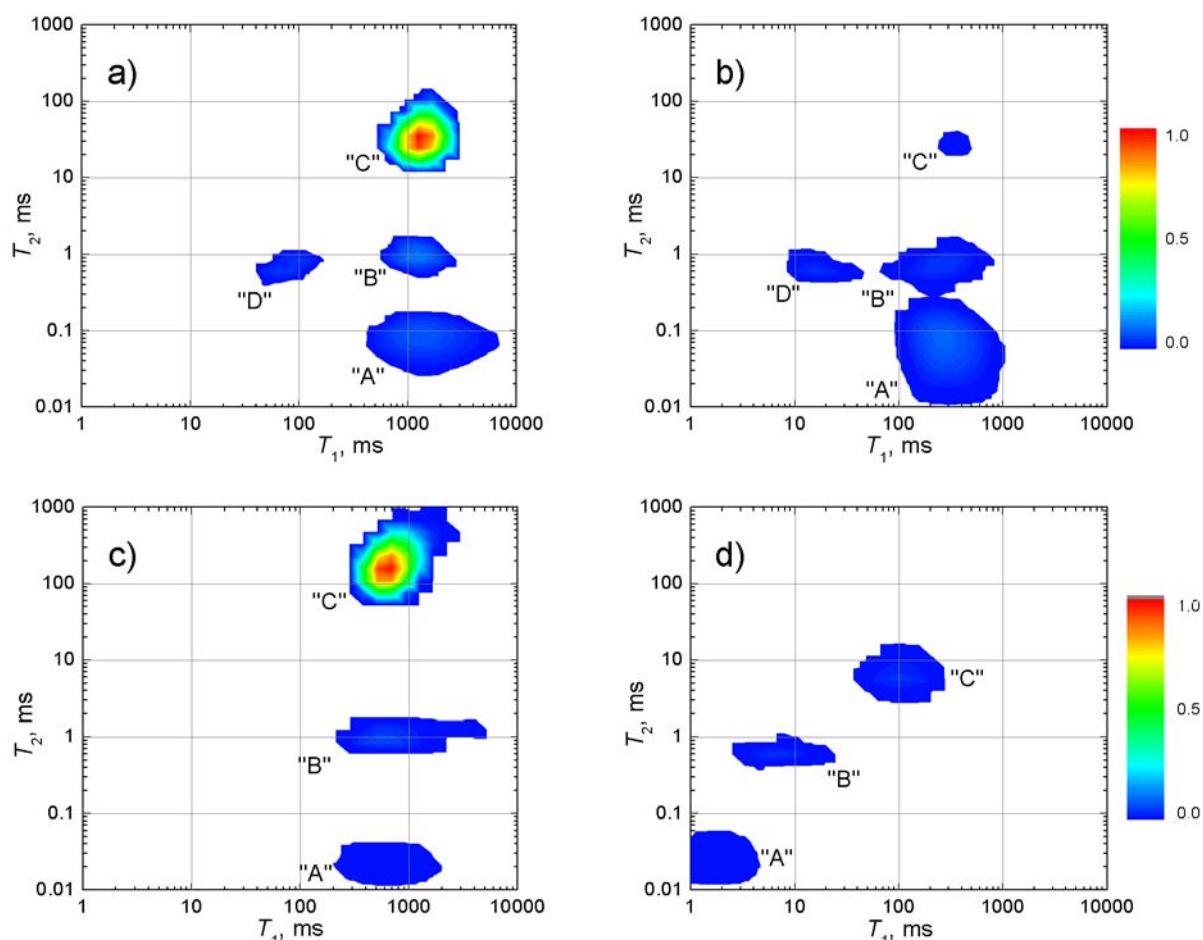
**Figure 3.** $T_1$-$T_2$ correlation maps of n-hexane (a, b) and water (c, d) in silicalite-1 at full (a, c) and partial saturations (b, d). The capital letters note corresponding peaks (see in text).

Regarding the sample of silicalite-1 partially saturated with n-hexane, the same $T_1$ and $T_2$ components in NMR signal are observed (Figure 3b). However, values of $T_1$ and $T_2$ are much lower than ones in fully saturated sample. Moreover, there is a difference in relative intensities of the observed components in fully and partially saturated silicalite-1. Consequently, it indicates that in fully saturated sample almost all adsorbed volume (>98%) of n-hexane is in channels ("A" peak) and mesopores ("B" and "D") of silicalite-1. Relative intensities of these peaks are also in good agreement with Brunauer-Emmett-Teller (BET) data and values of relative intensities obtained for the fully saturated sample. A weak "C" peak comes from the intercrystallite volume of silicalite-1 similarly to the fully saturated sample.

The NMR signal from water in intracrystallite channels is presented by "A" peak with $T_2 \approx 30$ μs (Figure 3d). However, a relative intensity of the peak "A" is much lower than that in the n-hexane saturated sample (Figure 3b). It might suggest that the high hydrophobicity of silicalite-1 channels prevents the penetrating of water molecules into silicalite-1 at least at normal conditions. Note that this property is used in membranes based on silicalite-1 to separate water and alcohol in binary mixtures [25].

The water molecules with shortest relaxation time adsorbed in silicalite-1 are characterized by a transverse relaxation time $T_2 \sim 30$ μs and a relative part in the whole NMR signal of $\sim 4\%$ in the partially saturated and <1% in the fully saturated samples, correspondingly. This $T_2$ value is less than $T_2 \sim 80$ μs observed in molecules of n-hexane saturated samples located in silicalite-1 channels. We suggest that defects and other imperfections of the silicalite-1 intracrystallite channels supply adsorption sites for water molecules. Whereas for these sites located in hydrophobic intracrystallite channels, there are stronger restrictions of molecular mobility for water than for n-hexane. It leads to a higher decrease of $T_2$ values for water. The defects of silicalite-1 crystal structure also may lead to forming of hydroxyl

groups on the surface, which will cause an increasing in the hydrophilic properties of the surface in silicalite-1 [10] and adsorption energy for water molecules consequently.

Only peaks parallel to the diagonal are observed on the $T_1$-$T_2$ map of water in silicaite-1 at partial saturation of porous volume (Figure 3d). The absence of cross peaks and the presence of different values of $T_1$ for different components of NMR signal indicates that measured values of relaxation times are not corrupted by exchange.

## *Molecular exchange in silicalite-1 by 2D $T_2$-$T_2$ NMR*

As mentioned earlier the presence of cross-peaks on the $T_1$-$T_2$ maps and differences in values of relaxation times could be explained as a result of the exchange processes which corrupts both experimental values of relaxation times and relative amplitudes of different components of NMR signal. The single value of $T_1$ instead of broad $T_1$ distribution for molecules adsorbed in different parts of porous volume also indicates the presence of magnetization exchange between different parts of silicalite-1 porous volume. The processes of magnetization transfer in this system are most likely attributed to molecular exchange by self-diffusion [26, 27].

The values of relaxation times specify a fast exchange regime in scale of $T_1$ times, i.e. the exchange time less than ~100 ms. However, in scale of $T_2$ times the exchange between these three sites might be in different regimes. In this study it is suggested that duration of exchange between different components are not significantly less than values of $T_2$ of corresponding components which assumes slow or intermediate exchange rate limit. In this case only exchange effect is assumed as a source of change of cross-peak intensities in $T_2$-$T_2$ exchange experiment. However, more precise information can be obtained from simulation of $T_2$-$T_2$ maps considering both relaxation and exchange effects on intensity of cross peaks [28, 29].

The ^{1}H 2D $T_2$-$T_2$ exchange NMR of adsorbed liquids in silicalite-1 was measured in the range of mixing times 0.02-320 ms. Further increasing of mixing time leads to prevailing of $T_1$-weighting effects. Example of 2D exchange maps of n-hexane at full and partial saturation of silicalite-1 are presented in Figure 4. It is clear that there are three (Figure 4a) and two (Figure 4b) sites in silicalite-1 porous volume for molecular exchange with n-hexane fully and partially saturated respectively.

The relatively symmetrical cross-peaks patterns on $T_2$-$T_2$ exchange map allow to assume that exchange between two different components is going independently without involving of third component. Thus processing of resulted data in the case of three site exchange is simplified by analysis integral intensities of cross-peaks. Experimental dependencies of the cross-peak intensities with mixing time $t_{\text{mix}}$ are presented in Figure 5. The corresponding exchange times $\tau_{\text{exch}}$ (see Table 1) was obtained from fitting experimental data by function:

$$A_{\text{cp}}(t_{\text{mix}}) = A_0 \exp\left(-\frac{t_{\text{mix}}}{T_1}\right)\left[1 - \exp\left(-\frac{t_{\text{mix}}}{\tau_{\text{exch}}}\right)\right]. \tag{5}$$

Accordingly, the exchange time is calculated from time mixing dependency of integral intensity of cross peaks by means of the non-negative least square method using Eq. (5) with $T_1$ values obtained from $T_1$-$T_2$ experiments.

The absence of reliable results for "B-C" and "A-C" peaks exchange is due to low intensity of "C" peak in the partially saturated silicalite-1 sample with n-hexane. In the partially saturated sample with water no cross-peaks were observed because of prevailing of $T_1$-relaxation as it follows from the $T_1$-$T_2$ maps. Therefore the values of exchange time for water are presumably longer than corresponding values of $T_1$ and $T_2$ relaxation times.

Since exchange time between channels and intercrystallite pore volumes ("A-C" peaks exchange) can depend on size of silicalite-1 crystallites, it is possible to estimate a self-diffusion coefficient by [24]:

$$t_{\text{exch}} = r^2/15D, \tag{6}$$

where $r$ is a size of exchangeable domain, $D$ is a self-diffusion coefficient and $t_{\text{exch}}$ is the exchange time.
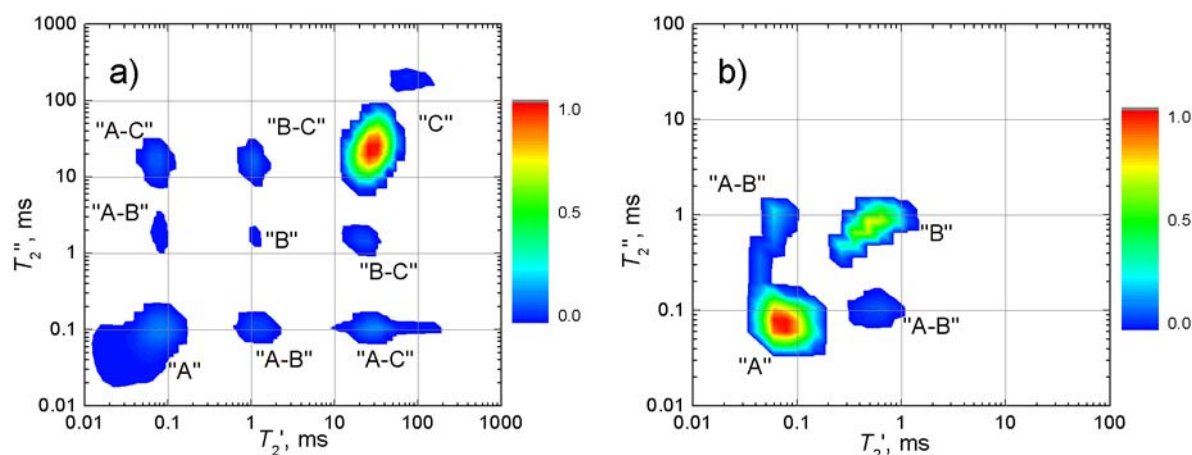
**Figure 4.** $T_2$-$T_2$ maps of n-hexane in silicalite-1 at full (a) and partially (b) saturated sample. Mixing time is 10 ms and 2 ms correspondingly.
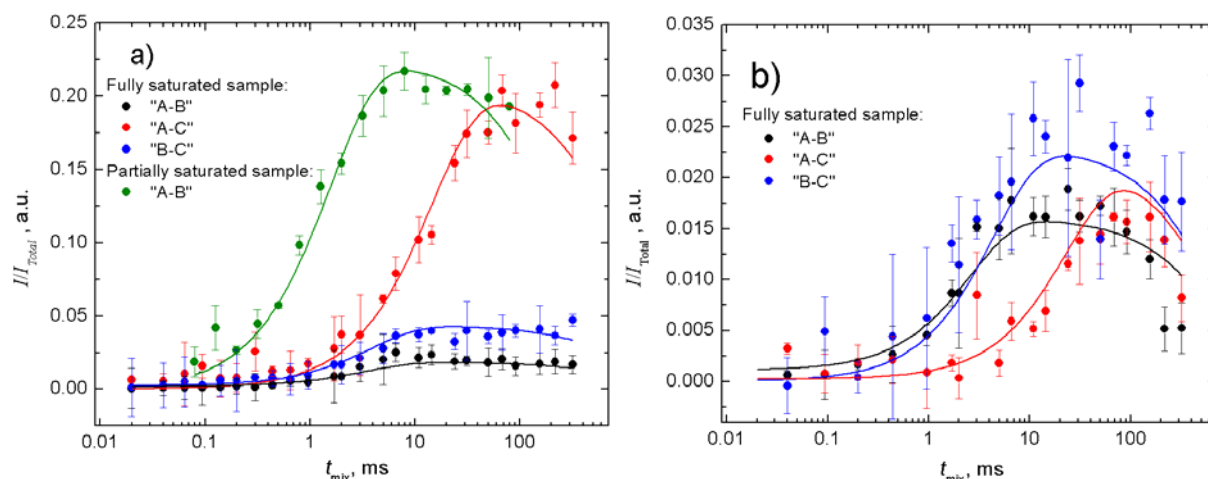


**Figure 5.** Time dependences of relative part of diagonal peaks ("A-C", "B-C", "A-B") in the exchange correlation maps of n-hexane a) and b) water in silicalite-1. Solid lines present fitting by Eq. (5).

**Table 1.** Exchange times obtained from fitting of experimental data with Eq. (5).

| Liquid | Saturation | Exchange time, ms | | |
|---|---|---|---|---|
| | | "A-B" | "B-C" | "A-C" |
| n-hexane | full | $3.3 \pm 0.58$ | $3.9 \pm 0.22$ | $15.01 \pm 1.41$ |
| | partial | $1.6 \pm 0.16$ | - | - |
| water | full | $2.63 \pm 0.44$ | $4.5 \pm 0.52$ | $25 \pm 3.51$ |

Using 5 µm as a typical size of crystallites the values of the self-diffusion coefficient of $1.11 \times 10^{-10}$ and $6.67 \times 10^{-11}$ m²/s were obtained for n-hexane and water, respectively. The obtained values are in good agreement with literature data [10, 26, 30]. However it should be noted that direct measurement of self-diffusion coefficients of molecules in the silicalite-1 channels by NMR PFG is complicated because of very short $T_2$ times.

Obtained values of self-diffusion coefficient of molecules in channels allows to estimate a distance between mesopores in silicalite crystallites by the same approach with Eq. (6) and values of "A-B" exchange time between channels and mesopores. The obtained value of $2.3 \pm 0.2$ µm for n-hexane is in good agreement with the assumption that possible source of mesopores is defects inside the crystallites

formed in the process of synthesis [31]. However a distance between mesopores obtained for silicalite-1 saturated by water is $1.6 \pm 0.1$ μm which is less than value obtained for n-hexane. As it was shown above the relative intensity of the "A" peak corresponding to water molecules in channels on $T_1$-$T_2$ map is much less than the one in samples with n-hexane. Moreover, a nanopore volume estimated by BET [10] indicates a low saturation of channels with water. According to this result we suggest a non-uniform distribution of water molecules preferably close to the mesopores in silicalite-1. Furthermore, it leads to a short estimated distance between mesopores. On the other hand, in the case of partially saturated silicalite-1 with n-hexane the estimated distance between mesopores of $1.63 \pm 0.08$ μm is also less than the one in fully saturated samples. The values of relative intensity of peaks and absolute NMR signal normalized to weight of silicalite-1 indicate an almost full filling of both channels and mesopores according to BET data. Thus the possible reason of the observed effect might be the molecular exchange involving gas phase from intercrystallite pore volume that accelerates a transfer of n-hexane molecules between different part of silicalite-1.

## 4. Summary

The molecular exchange of n-hexane and water between different pore volumes in silicalite-1 was studied by means of two dimensional ^{1}H NMR relaxometry. The combined acquisition method including FID and CPMG decay was applied to measure in wide range of the ^{1}H nuclear longitudinal and transverse relaxation times of adsorbate n-hexane and water molecules in silicalite-1. Obtained data provides information about state and behavior of adsorbate molecules in silicalite-1 porous volume.

It was determined that the molecular exchange in fully saturated silicalite-1 with n-hexane and water could be characterized by three sites. Analyzing relaxation times and relative parts of relaxation components in ^{1}H NMR signal, it was suggested that porous volume in silicalite-1 is presented by three types of pores, namely intracrystallite (channels) pores, mesopores and intercrystallite pores in free space between powder particles. The estimated exchange times were found in a good agreement with literature data. Also good agree was found between estimated and experimentally defined values of self-diffusion coefficients. The sizes of exchangeable domains estimated from exchange times of n-hexane and water in silicalite-1 were defined as $2.3 \pm 0.2$ and $1.6 \pm 0.1$ μm for fully saturated samples, correspondingly. The absence of significant adsorption of water molecules in channels is explained by hydrophobicity of channels, whereas mesopores and defects in crystalline structure can form the hydrophilic sites for adsorption of water molecules.

## Acknowledgments

## References

1. Krishna R., Smit B., Vlugt T.J.H. *J. Phys. Chem. A* **102**, 7727 (1998)
2. Funke H.H., Argo A.M., Falconer J.L., Noble R.M. *Ind. Eng. Chem. Res.* **36**, 137 (1997)
3. Kapteijn F., Bakker W.J.W., van de Graaf J., Zheng G., Poppe J., Moulijn J.A. *Catalysis Today* **25**, 213 (1995)
4. Chen N.Y., Kaeding W.W., Dwyer J. *J. Am. Chem. Soc.* **101**, 6783 (1979)
5. Christensen C.H., Johannsen K., Törnqvist E., Schmidt I., Topsøe H., Christensen Ch.H. *Catalysis Today* **128**, 117 (2007)
6. Kärger J., Demontis P., Suffritti G.B., Tilocca A. *J. Chem. Phys.* **110**, 1163 (1999)
7. Vasenkov S., Bo1hlmann W., Galvosas P., Geier O., Liu H., Kärger J. *J. Phys. Chem. B* **105**, 5922 (2001)

8. Caro J, Bülow M., Kärger J., Pfeifer H. *J. Catal.* **114**, 186 (1988)

9. Takaba H., Yamomoto A., Hayamizu K., Oumi Y., Sano T., Akiba E., Nakao Sh. *Chem. Phys. Lett.* **393**, 87 (2004)

10. Filippov A., Dvinskikh S.V., Khakimov A., Grahn M., Zhou H., Furo I., Antzutkin O.N., Hedlund J. *Magn. Res. Imag.* **30**, 1022 (2012)

11. Kärger J, Pfeifer H, Heink W. *Principles and Application of Self-Diffusion Measurements by Nuclear Magnetic Resonance. Advances in Magnetic Resonance*, Academic Press, New York, Vol. **12**, p. 1 (1988)

12. Olson D.H., Kokotailo G.T., Lawton S.L., Meler W.M. *J. Phys. Chem.* **85**, 2238 (1981)

13. Noack M., Mabande G.T.P., Caro J., Georgi G., Schwieger W., Kolsch P., Avhale A. *Micropor. Mesopor. Mater.* **82**, 147 (2005)

14. Noack M.M. *Chem. Eng. & Tech.* **25**, 221 (2002)

15. Groen J.C., Peffer L.A.A., Moulijn J.A., Perez-Ramirez J. *Micropor. Mesopor. Mater.* **69**, 29 (2004)

16. Zhang L., van Laak A.N.C., de Jongh P.E., de Jong K.P. *Zeolites and Catalysis: Synthesis, Reactions and Applications*, edited by Čejka J., Corma A., Zones S. (Wiley-VCH Verlag CmbH & Co. KGaA 2010)

17. Mostowicz R, Crea F, Nagy J. *Zeolites* **13**, 678 (1993)

18. Song Y.-Q. Venkataramanan L., Hürlimann M.D., Flaum M., Frulla P., Straley C. *Jour. Magn. Reson.* **154**, 261 (2002)

19. Washburn K.E., Anderssen E., Vogt S.J., Seymour J.D., Birdwel J.E., Kirkland C.M., Codd S.L. *J. Magn. Reson.* **250**, 7 (2015)

20. Washburn K.E., Callaghan P.T. *Phys. Rev. Lett.* **97**, 175502 (2006)

21. Doroginitsky M.M. *Proceedings of the VII All-Russian Conference "Structure and Dynamics of Molecular Systems", Moscow*, p.50, (2000)

22. Tikhonov A.N., Arsenin V.Y. *Solution of III-posed Problems*, Winston & Sons, Washington (1977)

23. Baerlocher Ch., Meier W.M., Olson D.H. *Atlas of Zeolite Framework Types*, Elsevier, Amsterdam (2001)

24. Uryadov A.V., Skirda V.D., *Magn. Res. Imag.* **19**, 429 (2001)

25. Saravanan V., Waijers D.A., Ziari M., Noordermeer M.A. *Biochem. Eng. J.* **49**, 33 (2010)

26. Neudert O., Staps S., Mattea C. *J. Magn. Reson.* **208**, 256 (2011)

27. Paciok E., Haber A., Van Landeghem M., Blümich B. *Z. Phys. Chem.* **226**, 1243 (2012)

28. Van Landeghem M., Haber A., d'Espinose de Lacaillerie J.-B., Bluemich B. *Concepts in Magn. Res. A* **36A**, 153 (2010)

29. Johnson D.L., Schwartz L.M. *Phys. Rev. E* **91**, 062406 (2015)

30. Humplik T., Raj R., Maroo S.C., Laoui T., Wang E.N. *Langmuir* **30**, 6446 (2014)

31. Tao Y., Kanoh H., Abrams L., Kaneko K. *Chem. Rev.* **106**, 896 (2006)